Available online at www.sciencedirect.com
SCIENCE DIRECT
Sensors and Actuators A 120 (2005) 134–141
SENSORS AND ACTUATORS A PHYSICAL
www.elsevier.com/locate/sna

Structure and characterization of a planar normally closed bulk-micromachined piezoelectric valve for fuel cell applications

Hengbing Zhao[a,*], Kevin Stanley[a], Q.M. Jonathan Wu[b], Eva Czyzewska[a]

[a] *Department of Microtechnology and Sensing, Institute for Fuel Cell Innovation, 3250 East Mall, Vancouver, BC, Canada V6T 1W5*
[b] *Department of Electrical and Computer Engineering, University of Windsor, 401 Sunset Avenue Windsor, ON, Canada N9B 3P4*

Received 15 June 2004; received in revised form 19 November 2004; accepted 26 November 2004
Available online 7 January 2005

Abstract

Microfuel cell systems require microvalves that are chemically tolerant of hydrogen, have thermally insensitive activation mechanisms, and tight geometric constraints. A planar bulk-micromachined piezoelectric valve for portable fuel cell system is proposed. The actuating diaphragm and the valve seat are etched on silicon wafers. A piezoelectric bimorph disc is glued to the actuating diaphragm to lift the diaphragm and open the valve. The pressure differential between the valve chamber and the outlet and the initial pressure caused by the deformed tethers are employed to increase the sealing force. The actuating device with four Z-tethers attached to the actuating diaphragm is thermally insensitive and can reduce thermally induced deflection at the center and avoid clamping effect at circumferential edge. The proposed actuating diaphragm with Z-tethers shows good thermal stability and excellent actuating performance through the finite element method (FEM) analyses. The prototype valve of 20 mm in diameter and 2 mm thick was fabricated and tested as a regulator. Using compressed air, the flow characteristics for the prototype valve were measured at different inlet pressure and elevated air temperature. The design, fabrication, simulation and characterization of the prototype valve are described.

Keywords: Fuel cell system; Piezoelectric; Bulk-micromachining; Microvalve

1. Introduction

Small fuel cell systems are becoming promising candidates for commercial applications due to potentially high energy density. Efficient operation of fuel cells depends on the fuel flow rate, pressure and concentration [1–6]. The relevant microfluidic control components must be small to reduce the impact of balance of plant on the microfuel cell gravimetric and volumetric energy density, and at the same time meet fuel cell application requirements such as hydrogen tolerance, thermally insensitive activation and geometric constraints. Our goal is to develop a planar proportional valve and put it on the fuel line of a 20 W fuel cell system to control the fuel flow rate. The requirements are that operating temperature range is 10–85 °C, humidity is 0 RH to saturation, maximum flow rate is 350 sccm and pressure drop across the valve is 0–44.1 psi.

Various active microvalves have been developed so far [7–20]. There are four principal means that have been commonly utilized for microvalve applications: electrostatic forces [7], piezoelectric forces [8–14], shape memory alloys [16,17], and thermal expansion forces [18–20]. The piezoelectric actuation of microvalve structure is attractive due to the relative simplicity of the actuator design, scalable geometry, lower power consumption in static operations, rapid response, and high work energy density. Based on the above advantages of piezoelectric actuation and the requirements of small fuel cells, a planar normally closed piezoelectric valve was proposed. The microvalve is fabricated on silicon wafers using bulk-micromachining techniques and actuated by piezoelectric bimorph disc. Both silicon and piezoelec-

* Corresponding author. Tel.: +1 6042213000x5594; fax: +1 6042213001.
E-mail addresses: hengbing.zhao@nrc.ca (H. Zhao), jwu@uwindsor.ca (Q.M. Jonathan Wu).

0924-4247/$ – see front matter.
doi:10.1016/j.sna.2004.11.037

tric ceramic are hydrogen compatible. With Z-tethers design, the valve is thermally insensitive and can operated within relatively large temperature range. This paper describes the structure and the fabrication process of the valve. The simulation and test of thermal deflection and the behavior of the piezoelectric actuating device are presented. The flow rate and leak characteristics of the prototype valve are obtained.

2. Microvalve structure, fabrication and operation

Almost all applications of piezoelectric actuators in the microvalve can be grouped into two major areas: one where actuators are bonded on structures for flexural control by using the transverse effect – d_{31} piezoelectric strain coefficient of the material [8,9], and another where actuators are directly used for micropositioning as linear actuators by using the longitudinal effect – d_{33} piezoelectric strain coefficient [10–13].

Longitudinal piezoelectric effect can generate tremendous force. However, the stroke permitted by induced strain levels is miniscule, and requires amplification of the stroke of piezoelectric actuators [11,12]. The requirement for fabrication is also critical [10,13]. In our application, large deflection is required and low force can be tolerated. Therefore, the bimorph PZT element—transverse effect is utilized.

2.1. Structure

A schematic of the microvalve is shown in Fig. 1. The stand-alone device has a square footprint of 25 mm on a side, and a height of less than 2 mm. The valve consists of four parts: seat plate, actuating diaphragm, piezoelectric disc and top cover. The seat plate is known as the base, which may be part of the chamber wall. It contains the outlet, seal rings, and support spokes around the outlet. These rings tend to increase the sealing area and decrease gas leaks. The middle layer is the actuating diaphragm, which is patterned and etched on a silicon wafer and is connected to the border by four flexible Z-tethers, covering the valve seat. The four Z-tethers at the circumference of the actuating diaphragm are used to support the actuating diaphragm, increasing the flexibility at the contact line to avoid clamping effects, and reducing the thermal deflection at the center.

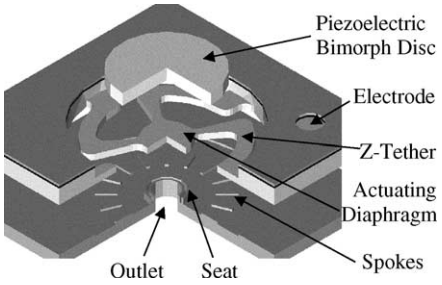

Fig. 1. Schematic view of the piezo valve without cover (not in scale).

The detailed dimensions and material parameters are given in the next section. The piezoelectric bimorph disc actuator is glued to the top of the diaphragm, and the electrodes are routed through the conducting layers of the actuating diaphragm.

For the prototype of the microvalve, a series bimorph with silver electrodes was employed. The bimorph element consists of two thin PZT plates (BM532, Sensor Tech.)—7 mm in radius and 0.25 mm thick, which were bonded together without internal shim. BM532 is a kind of PZT-5H materials from Sensor Technology Ltd. The electrode can be patterned and routed through different areas or layers of the actuating diaphragm and aligned with the wrap-around silver electrodes of the actuator. The disc bends out when a voltage is applied to the electrodes. If disc actuators are fixed at their circumferences, the center's motion can be used for actuating purposes.

2.2. Fabrication

A wet bulk-micromachining process is used to craft the structure on silicon wafer and simply explained here. First a thin oxide is thermally grown on the surface of silicon wafer. Then deposit positive/negative photoresist by spin coating or spraying. Expose to UV light by projection through film mask and immerse in an aqueous developer solution to dissolve exposed/unexposed resist. The pattern is transferred from film mask onto resist layer. Etch the exposed oxide to transfer the pattern to oxide layer and then remove the rest of resist. The patterned oxide is used as a mask against etching. Thus, etching can selectively remove material from a wafer.

Fig. 2 illustrates a schematic view of the fabrication process used for the prototype valve. The actuating diaphragm shown in Fig. 2a was made by patterning of the thermally grown oxide (1) on a double-sided polished 0.5 mm thick ⟨1 0 0⟩ p-type silicon wafer and etching of the cavity (2) and electrode hole (3) to the depth of 300 μm (tetraammoniumhydroxide (TMAH), 95 °C; 3 h 10 min). In the next step, boron was thermally diffused to form electrodes (4) (solid boron diffusion sources, 1000 °C; 45 min). Finally, supporting tether and boss (5) (details shown in Fig. 1) were etched through from the other side of the wafer (TMAH, 95 °C; 2 h 25 min).

The seat plate shown in Fig. 2b was fabricated using thermally oxidized single-sided polished ⟨1 0 0⟩ p-type silicon wafer. The first 20 μm deep alignment pattern (6) was etched using TMAH (95 °C; 30 min), followed by valve seat (o.d. 1.4 mm) etch (7) to the depth of 7.5 μm (TMAH 95 °C; 7 min). The wafer was then thermally oxidized to form a 0.5 μm thick SiO_2, that was next patterned and etched to form a 95 μm high spoke support (8) (TMAH 95 °C; 105 min). Final steps included etching sealing rings (9) (TMAH, standard conditions, 10 min), followed by laser drilling of 0.8 mm in diameter outlet (10) in the middle of the valve seat.

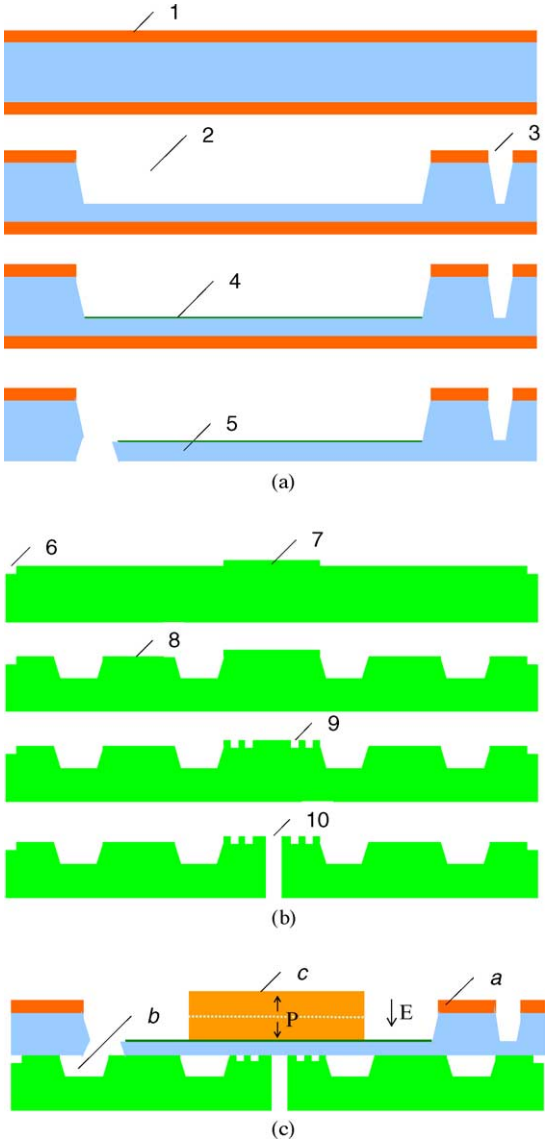

Fig. 2. Fabrication process (not in scale).

After aligning and gluing piezo bimorph disk *c* to the actuating diaphragm *a* with high-strength conductive epoxy (CW2400, Chemtronics) and attaching it to the seat plate *b* with thin epoxy-based adhesive, at the circumference in such a way that it covers the outlet (10), fabrication of the valve was completed. Fig. 2c shows a cross-section of the assembled valve. Here, P and E indicate the polarization direction of the bimorph disc and the direction of the applied electric field, respectively.

2.3. Operation

The valve is normally closed. The actuating diaphragm is forced in contact with the bottom plate in the outmost area and the central part of the actuating diaphragm is against the valve seat, making it slightly convex, and generating a sealing force on the outlet due to the deformation of the four tethers.

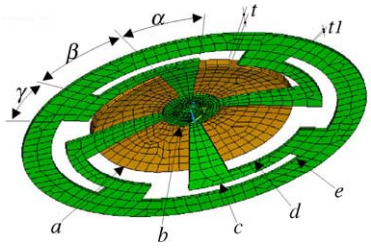

Fig. 3. Simulated bending mode of the actuating device. *t* and *a*: thickness and radius of the bimorph disc; *t*1, *c*, *d*: thickness, outer and inner radii of partial annulus of Z-tethers; α, β, γ: angles of a sector and two partial annuli of Z-tethers; *b*: radius of the central poppet; *e*: inner radius of valve chamber.

The initial sealing force can be controlled through adjusting the height of the valve seat. The pressure differential between the chamber and the outlet is exploited to increase the sealing force.

Here the series bimorph disc is employed as an actuating element. When a voltage is applied to the electrodes, the disc polarized in a direction consistent with the electric field will contract, and the disc polarized in the opposite direction will expand, causing the bimorph disc to bend out. The simulated bending mode of the actuating device is shown in Fig. 3. This creates a cylindrical channel between the actuating diaphragm and the valve seat, allowing for the passage of gases. Since gas flow is extremely sensitive to the height of the gap, the flow rate can be regulated by controlling the height of the cylindrical channel [21].

3. Analyses and characterization

The actuating diaphragm was designed and optimized at the contact line to decrease the deflection due to thermal expansion, avoid clamping effects at the circumferences, and at the same time amplify the piezoelectric deflection at the center. The detailed material and geometric parameters are tabularized in Table 1 for the following analyses.

Table 1
Material (BM532) and geometric parameters of the actuating device

K_3^T	3250
g_{31} (V m/N)	-7.5×10^{-3}
d_{31} (C/N)	-250×10^{-12}
Y_{11}^D (N/m^2)	7.14×10^{10}
δ (°C^{-1})	4×10^{-6}
a (mm)	7
t (mm)	0.5
b (mm)	2
c (mm)	9
d (mm)	8
e (mm)	10
*t*1 (mm)	0.2
α, γ (°)	20
β (°)	30
V (V)	150

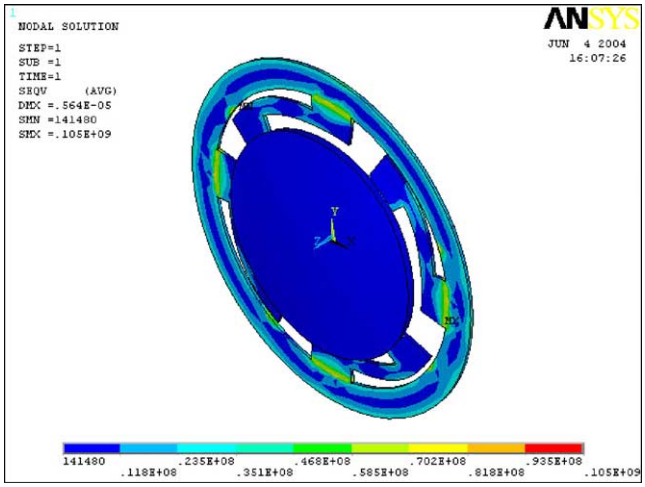

Fig. 4. Thermal deformation and stress distribution of an actuator with Z-tethers at 120 °C.

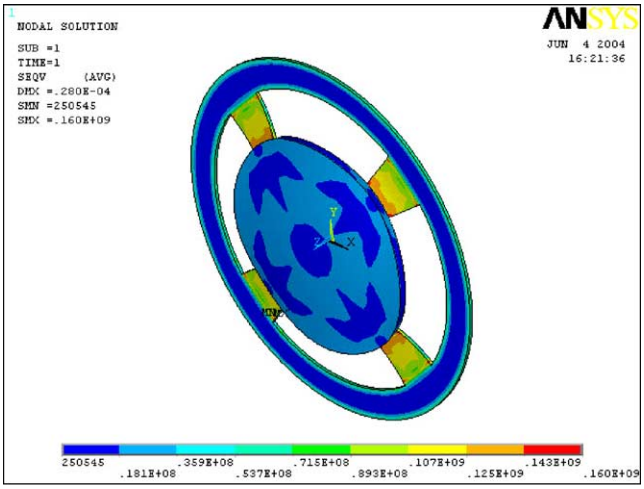

Fig. 5. Thermal deformation and stress distribution of an actuator with straight tethers at 120 °C.

3.1. Thermal analysis

Each piezoelectric material has a particular operating limit for temperature, voltage and stress. Operating a material over these limitations may cause partial or total depolarization of the material, and a diminishing or loss of piezoelectric properties. A temperature change of 75 °C (between 10 and 85 °C) is normal for PEM fuel cells. These temperature changes produce thermal strain and thermally induced deflections. The difference in thermal expansion coefficients δ between two joined layers of dissimilar materials will also cause bending to one side from a change in temperature. This deformation introduced by temperature change has significant effect on the operation of membrane valve. The FEM model in Fig. 3 was performed to analyze thermal deflection and stress distribution on the actuating device of the valve by using ANSYS Multiphysics (Release 8.0). Solid5 element with six degrees of freedom (magnetic, thermal, electric, and structural) at each node was employed. The actuator made of piezoelectric bimorph and silicon elastics was analyzed neglecting the effects of the thin adhesive layer for simplification.

Thermal deflection in *z*-direction (normal direction) and thermal stress distribution were obtained for the actuating device with Z-tethers and straight tethers. Figs. 4 and 5 give the deformed shape and the stress distribution of the actuator with Z-tethers and straight tethers at 120 °C, respectively. Fig. 6 gives the maximum deflection D in *z*-direction and the maximum stress S of the actuator with Z-tethers and straight tethers. Compared to the straight tethers, the Z-tethers can reduce the thermally induced deflection in *z*-direction to one fifth and the mechanical stress to two-thirds. The Z-tether structure cannot decrease the deflection in z direction caused by the mismatch of coefficient of thermal expansion of piezoceramics and silicon. But it can accommodate the expansion in radial direction and avoid converting the radial expansion into the *z*-directional deflection. With the Z-tether design it is possible to operate the valve over a relatively wide temperature range, without considering compensating thermal deformation by applying some additional voltage to the piezo disc.

3.2. Deflection and blocking force

Although the finite element method (FEM) and experimental techniques can be used to characterize the piezoelectric actuators, analytical models that predict the response of the actuators are helpful in understanding the effects of various parameters on the predicted response and also in optimizing the performances of the device. Neglecting the elements of electrical and mechanical energy dissipation for simplicity, the electromechanical equivalent circuit of circular bimorph [22–28], as shown in Fig. 7, is used to derive the input–output relationships between the electrical and mechanical terminals.

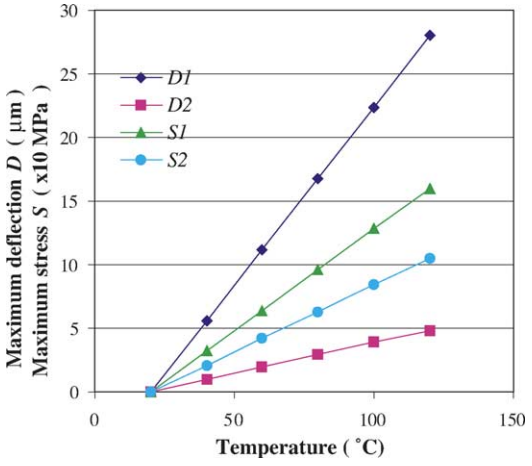

Fig. 6. Comparison of thermal deflection and stress of actuators with straight and Z-tethers.

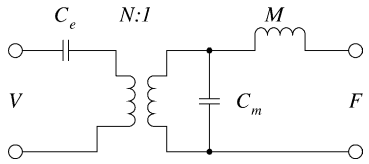

Fig. 7. Electromechanical equivalent circuit. C_e is the free electrical capacitance, N is the transducer ratio, C_m is compliance under open circuit conditions, V is the applied voltage, F is the applied force, and M is the effective mass.

Operation below resonance and a simply supported disc with a concentrated load at the center are assumed. For this case, the maximum free deflection D_f and the blocking force F_b at the center can be obtained by shortening and opening the mechanical terminal of the equivalent circuit, respectively:

$$D_f = \frac{3d_{31}}{2}\left(\frac{a}{t}\right)^2 V \quad (1)$$

$$F_b \cong 3g_{31}K_3^T\varepsilon_0 Y_{11}^D tV \quad (2)$$

where a is the radius of bimorph disc, t the overall thickness of bimorph, K_3^T the free dielectric permittivity, Y_{11}^D the Young's modulus under the open-circuit condition, g_{31} the piezoelectric constant relating field developed to applied stress and d_{31} is the piezoelectric strain constant. From Eqs. (1) and (2), we can see that for a given voltage V the maximum deflection is determined by the ratio of the radius to the thickness, and the blocking force depends on the thickness of the bimorph disc. According to the above equations, a series BM532 bimorph disc with radius $a = 7$ mm and total thickness $t = 0.5$ mm can produce a blocking force of 3.5 N and a maximum deflection of 11.0 μm at the center under the applied voltage of 150 V.

The above blocking force and the deflection of the bimorph disc are considered with mechanically free boundary conditions. The generative deflection of a bimorph is decreased due to gluing to the actuating diaphragm and mechanically clamping at the circumferential edge and amplified due to increased radius of the diaphragm. Static and mode analysis were performed based on the parameters in Table 1. The maximum stroke of 10.5 μm and the opening force of 2.19 N at the center were obtained. The resonant frequency of the first bending mode is 3.656 kHz.

3.3. Deflection measurement

The actuating device was fabricated. Photographs of the etched valve seat plate, actuating diaphragm and its adhering surface, and assembled actuating device are shown in Fig. 8. The thickness of the diaphragm can be controlled exactly. The width of the partial annulus of the tether was greatly affected by underetching due to different etching rate at different direction. This has very limited effect on the deflection according to the simulation and will decease the sealing force greatly.

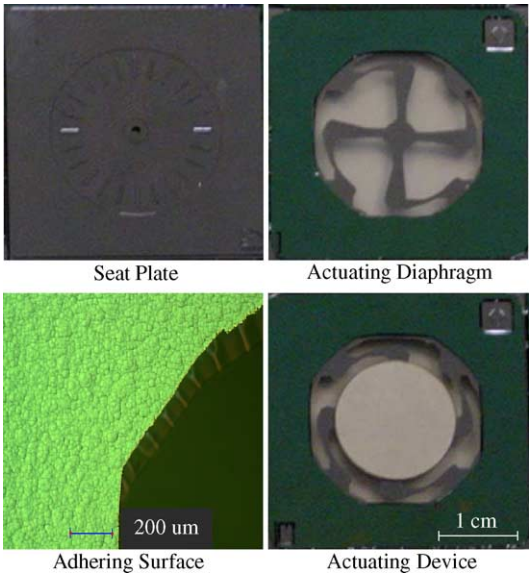

Fig. 8. Photograph of bulk-micromachined actuating diaphragm, bottom plate and actuating device.

To analyze the valve characteristics in detail, it would be useful to measure the deflection of the actuating diaphragm. The deflected actuating diaphragm was scanned with a WYKO 3D surface profiler at room temperature. Fig. 9 shows the scanned deformed profile of the diaphragm from the bottom. The color/gray scale shows the deflection in normal direction. The x and y deflection profiles show a high degree of symmetry. After several cycles of applied voltage from 0 to 180 V, the relationship between the applied voltage and the deflection becomes reproducible. The measured and simulated maximum deflection versus applied voltage is shown in Fig. 10 . With a proper input voltage, the distance between the actuating diaphragm and the valve seat can be controlled. Compared to the FEM result, an initial offset and hysteresis caused by the transition of the spontaneous polarization between the positive and negative directions are clear

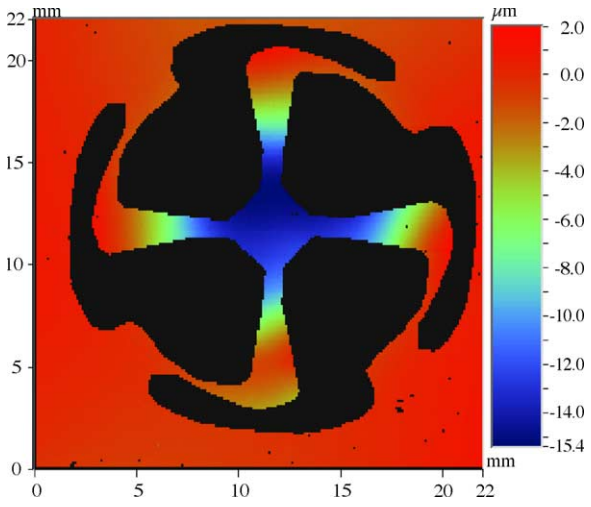

Fig. 9. Scanned 2D profile of the actuating diaphragm under 182 V voltage.

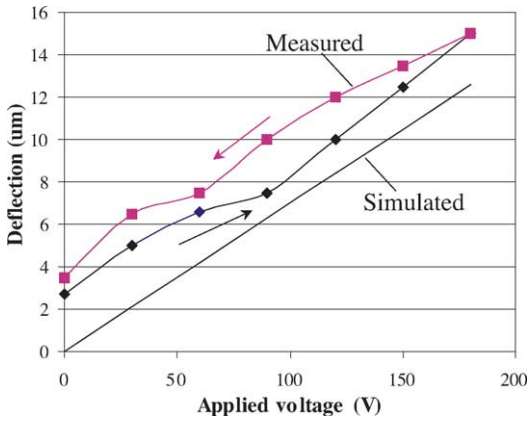

Fig. 10. Deflection in *z*-direction vs. applied voltage.

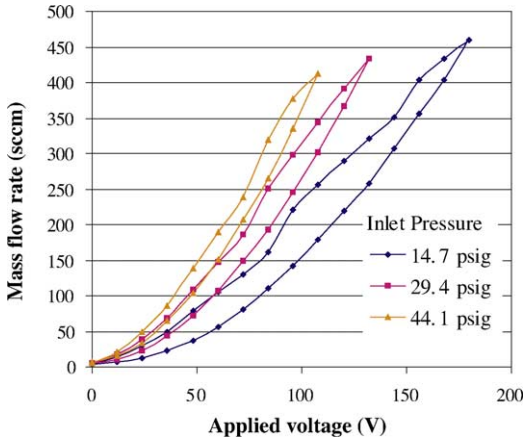

Fig. 12. Measured flow rate vs. applied voltage at different inlet pressure.

in the diagram. The polarization shows hysteresis with respect to the applied electric field. In the free state (no applied voltage), the deflection offset is approximately 3 μm, which appeared after the voltage was applied and was not introduced by the fabrication.

3.4. Flow characteristics

The valve without a top cover was fabricated and sandwiched into the test jig, so that the inlet and outlet holes can be easily accessed. The valve was tested as a regulator. Compressed air was supplied to the inlet of the valve at pressure of up to 46 psig. Air pressure at the inlet can be accurately adjusted using regulators. Air temperature can be controlled through a hot tube before the valve. A thermocouple near the inlet of the valve is used to monitor the air temperature. The inlet pressure, outlet pressure and the mass flow rate were measured and logged using digital pressure transducers and mass flow meter. Fig. 11 shows a schematic and photograph of testing apparatus.

The mass flow characteristics of the valve as a function of the applied voltage are shown in Fig. 12. The mass flow rate versus the applied voltage was measured at room temperature with the input air pressure of 14.7, 29.4, and 44.1 psig. The flow characteristics display the same narrow hysteresis as the deflection with respect to the applied voltage. With a proper input signal, the valve can operate as a proportional valve to regulate flow. The flow characteristics at the elevated air temperature of 30, 50 and 70 °C are given in Fig. 13. Except for a little shift of the flow rate, the valve shows good thermal stability. Fig. 14 shows the leakage flow through the prototype valve when the inlet pressure varies between 0 and 46 psig.

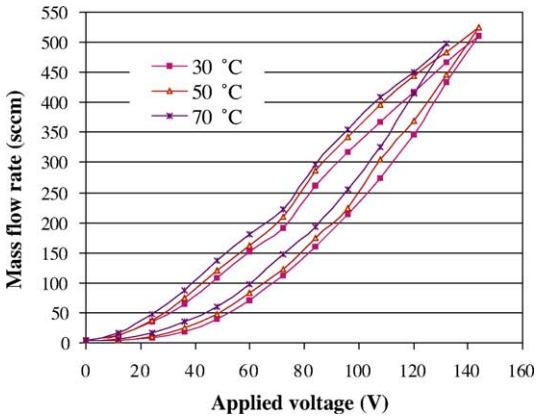

Fig. 13. Measured flow rate vs. applied voltage at different air temperature.

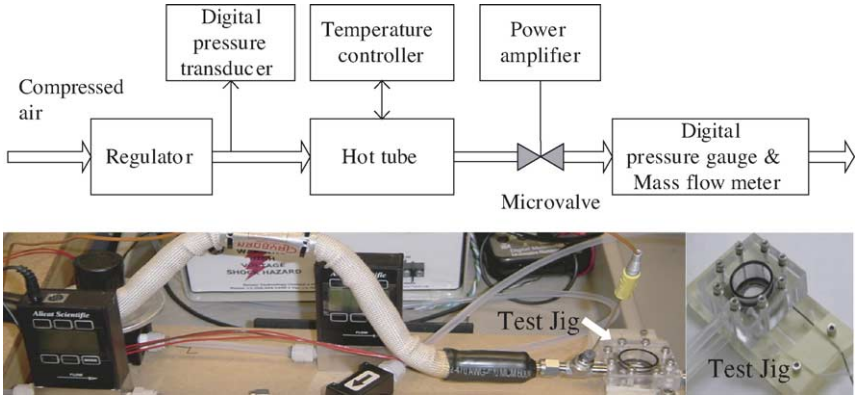

Fig. 11. Schematic and photograph of test setup.

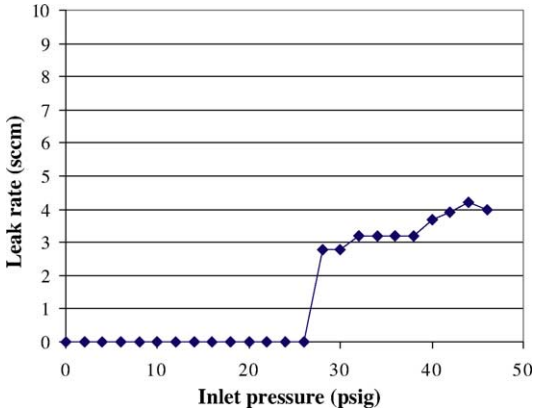

Fig. 14. Leak rate at inlet pressure up to 46 psig (room temperature).

The leak only occurs when the pressure drop across the valve is high, which may be caused by the deformation introduced by the pressure resulting from the asymmetries introduced into the structure during micromachining and fabrication.

4. Summary

A new planar normally closed bimorph actuated microvalve for microfuel cell system applications has been fabricated and tested. The actuating diaphragm and the valve seat were etched on silicon wafers. A piezoelectric bimorph disc was employed to drive the actuating diaphragm and open the valve. The whole valve is hydrogen compatible. The actuating diaphragm with four Z-tethers was proposed to reduce the clamping force, increase the actuating deflection, and reduce the thermally induced deflection. Compared to the actuating device with straight tethers, the proposed actuating diaphragm with Z-tethers shows good thermal stability and excellent actuating performance through FEM analyses. Finally, the prototype valve of 20 mm in diameter and 2 mm in thickness was fabricated and tested as a regulator at different inlet pressure and elevated air temperature. The valve worked well and showed good thermal stability. The flow rate and leak characteristics were obtained.

References

[1] B. Gurau, S.E. Smotkin, Methanol crossover in direct methanol fuel cells: a link between power and energy density, J. Power Sources 112 (2002) 339–352.
[2] D.r. Palo, J.D. Holladay, R.T. Rozmiarek, C.E. Guzman-Leong, Y. Wang, J. Hu, Y.-H. Chin, R.A. Dagle, E.G. Baker, Development of a soldier-portable fuel cell power system. Part 1. A bread-board methanol fuel processor, J. Power Sources 108 (2002) 28–34.
[3] J. Godat, F. Marechal, Optimization of a fuel cell system using process integration techniques, J. Power Sources 118 (2003) 411–423.
[4] M. Baldauf, W. Preidel, Experimental results on the direct electrochemical oxidation of methanol in PEM fuel cells, J. Appl. Electrochem. 31 (2001) 781–786.
[5] K. Scott, W. Taama, Performance of a direct methanol fuel cell, J. Appl. Electrochem. 28 (3) (1998) 289–297.
[6] H. Dohle, J. Mergel, D. Stolen, Heat and power management of a direct-methanol-fuel-cell system, J. Power Sources 111 (2002) 268–282.
[7] W. van der Wijngaart, H. Ask, P. Enoksson, G. Stemme, A high-stroke, high-pressure electrostatic actuator for valve applications, Sens. Actuators A 100 (2002) 264–271.
[8] J. Joswig, Active micromechanic valve, J. Micromech. Microeng. 2 (1992) 262–265.
[9] M. Koch, A.G.R. Evans, A. Brunnschweiler, Characterization of micromachined cantilever valves, J. Micromech. Microeng. 7 (1997) 221–223.
[10] I. Chakraborty, W.C. Tang, D.P. Bame, T.K. Tang, MEMS microvalve for space applications, Sens. Actuators 83 (2000) 188–193.
[11] D.C. Roberts, N.W. Hagood, Y.-H. Su, H. Li, J.A. Carretero, Design of a piezoelectrically driven hydraulic amplification microvalve for high pressure, high frequency applications, in: Proceeding of SPIE, The International Society for Optical Engineering, vol. 3985, 2000, pp. 616–628.
[12] H.Q. Li, D.C. Roberts, J.L. Steyn, K.T. Turner, O. Yaglioglu, N.W. Hagood, S.M. Spearing, M.A. Schmidt, Fabrication of a high frequency piezoelectric microvalve, Sens. Actuators A111 (1) (2004) 51–56.
[13] E. Hyeok-Eh, C. Lee, J. Mueller, Normally closed leak-tight piezoelectric microvalve under ultra-high upstream pressure for integrated micropropulsion, in: Proceedings of the IEEE 16th Annual International Conference on Microelectro Mechanical Systems, Kyoto, Japan, 2003, pp. 80–83.
[14] Shuxiang Dong, XiaoHong Du, Philippe Bouchilloux, Kenji Uchino, Piezoelectric ring-morph actuators for valve application, J. Electroceram. 8 (2002) 155–161.
[15] N. Vandelli, D. Wroblewski, M. Velonis, T. Bifano, Development of a MEMS microvalve array for fluid flow control, J. Microelectromech. Syst. 7 (4) (1998) 395–403.
[16] G. Hahm, H. Kahn, S.M. Philips, A.H. Heuer, Fully microfabricated, silicon spring biased, shape memory actuated microvalve, in: Solid-State Sensor and Actuator Workshop, 2000, pp. 230–233.
[17] M. Kohl, D. Dittmann, E. Quandt, B. Winzek, Thin film shape memory microvalves with adjustable operation temperature, Sens. Actuators 83 (2000) 214–219.
[18] M.A. Huff, M.S. Mettner, T.A. Lober, M.A. Schmidt, Fabrication, packaging and testing of a wafer-bonded microvalve, in: Solid-State Sensor and Actuator Workshop, 1992, pp. 194–197.
[19] H. Jerman, Electrically activated, normally-closed diaphragm valves, J. Micromech. Microeng. 4 (1994) 210–216.
[20] C.A. Rich, K.D. Wise, A high-flow thermopneumatic microvalve with improved efficiency and integrated state sensing, J. Microelectromech. Syst. 12 (2) (2003) 201–208.
[21] E.B. Arkilic, M.A. Schmidt, K.S. Breuer, Gaseous slip flow in long microchannels, J. Microelectromech. Syst. 6 (2) (1997) 167–178.
[22] S.K. Ha, Y.H. Kim, Analysis of an asymmetrical piezoelectric annular bimorph using impedance and admittance matrices, J. Acoust. Soc. Am. 110 (1) (2001) 208–215.
[23] S.K. Ha, Y.H. Kim, Impedance and admittance matrices of symmetric piezoelectric annular bimorphs and their applications, J. Acoust. Soc. Am. 108 (5) (2000) 2125–2133.
[24] Technical Publication TP-230, Circular Bender Bimorphs, Morgan Electro Ceramics.
[25] A. Ballato, Modeling piezoelectric and piezomagnetic devices and structures via equivalent networks, IEEE Trans. Ultrason. Ferroelectr. Freq. Contr. 48 (5) (2001) 1189–1240.
[26] S.K. Ha, Analysis of the asymmetric triple-layered piezoelectric bimorph using equivalent circuit models, J. Acoust. Soc. Am. 110 (2) (2001) 856–864.
[27] A.B. Dobrucki, P. Pruchnicki, Theory of piezoelectric axisymmetric bimorph, Sens. Actuators A58 (1997) 203–212.
[28] Kenji Uchino, Ferroelectric Devices, Marcel Dekker, 2000, pp. 77–80.

Biographies

Hengbing Zhao received the PhD degree in electrical engineering from Zhejiang University, China, in 1999. Then he worked on energy conversion and control in Japan until 2002. He is currently a research associate in Microtechnology and Sensing Group at the National Research Council Institute for Fuel Cell Innovation. His current research interests include microfluidic control and microfuel cell systems.

Kevin Stanley is currently leading the MicroFuel Cell Project at the National Research Council Institute for Fuel Cell Innovation in Vancouver, BC. He has received awards for innovation and leadership from the institute for this work. Mr. Stanley received his masters degree in 1997. He is currently completing his PhD at the same institution. Mr. Stanley's research interests include low cost microfabrication techniques, microsensing, microfluidics and microfuel cell systems.

Q.M. Jonathan Wu received the PhD degree in electrical engineering from the University of Wales, Swansea, UK in 1990. In 1995, he joined the National Research Council of Canada where he became a senior research officer and group leader. He is currently an associate professor in the Department of Electrical and Computer Engineering at the University of Windsor, Canada. He has published over 80 scientific papers in areas of computer vision, neural networks, fuzzy systems, robotics, micro-sensors and actuators, and integrated micro-systems. His current research interests include 3D image analysis, active video object extraction, vision-guided robotics, sensor analysis and fusion, wireless sensor network, and integrated micro-systems. Dr. Wu is serving as a General Co-Chair of the 2006 IEEE International Conference on Perception and Communication of Video and Graphics to be held in Vancouver, Canada. He is also an Associate Editor for IEEE Transaction on Sytems, Man, and Cybernetics (Part A).

Eva Czyzewska received her PhD degree in organic chemistry at the Polish Academy of Sciences in Warsaw, Poland in 1978. She worked at the Chemistry Department of Simon Fraser University from 1980 to 1992. She moved to SFUs School of Engineering Science in 1992. In 2001 she joined National Research Council of Canada. Her recent scientific interests include microfabrication and micromachining.